The work function of submonolayer cesium-covered gold: A photoelectron spectroscopy study

J. L. LaRue,[1] J. D. White,[1] N. H. Nahler,[1] Z. Liu,[2] Y. Sun,[2] P. A. Pianetta,[2] D. J. Auerbach, and A. M. Wodtke[1,a)]
[1]*Department of Chemistry and Biochemistry, University of California, Santa Barbara, California 93106-9510, USA*
[2]*Stanford Synchrotron Radiation Laboratory, Stanford, California 94309, USA*

(Received 9 May 2008; accepted 10 June 2008; published online 11 July 2008)

Using visible and x-ray photoelectron spectroscopy, we measured the work function of a Au(111) surface at a well-defined submonolayer coverage of Cs. For a Cs coverage producing a photoemission maximum with a He–Ne laser, the work function is 1.61 ± 0.08 eV, consistent with previous assumptions used to analyze vibrationally promoted electron emission. A discussion of possible Cs layer structures is also presented. © *2008 American Institute of Physics*. [DOI: 10.1063/1.2953712]

I. INTRODUCTION

Low work function solids have recently attracted interest in the field of nonadiabatic molecule-surface energy transfer due to the observation of vibrationally promoted electron emission.[1–4] In those studies, NO molecules with up to 3.65 eV vibrational energy were prepared in a molecular beam using stimulated emission pumping.[5] When these molecules collided with a solid surface whose work function was estimated to lie between 1.3 and 1.6 eV, electron ejection into the gas phase was observed. A vibrational threshold for electron emission near $E_{vib}=1.76$ eV, the energy for NO($v=8$), was taken as key evidence for direct conversion of molecular vibration to solid electronic excitation. The absence of electron emission signal for NO($v=7$), where $E_{vib}=1.55$ eV, was consistent with the estimated work function; however, an energetic "overshoot" could not be ruled out. It was pointed out that such an overshoot—of a few tenths of an eV—might be consistent with a postulated vibrational autodetachment mechanism[6] involving two electronically nonadiabatic electron transfer events.[3] Clearly, reducing the uncertainty associated with the work function to a value substantially less than the vibrational quantum level spacing in NO would be helpful to any efforts at obtaining a better understanding of the mechanism of vibrationally promoted electron emission.

In the work just mentioned, the low work function surface was obtained by exposing a Au(111) surface to a controlled dose of Cs while monitoring photoemission with a helium–neon (HeNe) laser.[2–4] During deposition, the work function decreases to a value below that of gold or cesium, an effect which is attributed to the dipolar layer induced by electron transfer from the alkali layer to the gold substrate. If alkali coverage is further increased, dipolar repulsion reduces the surface polarization and eventually a thick alkali film exhibits a work function typical of the pure alkali.[7] Dosing is ceased at the photoemission maximum as there is an approximate correlation between the work function minimum and the photoemission maximum observed in other alkali/metal systems.[8] For example, with Cs dosing experiments on W,[8] Ru,[9] and Ag,[10] the work function minima were found at

$$\mathrm{W}: \theta_{\mathrm{Cs}} \sim 2.5 \times 10^{14}\ \mathrm{Cs/cm^2}, \quad \Phi = 1.5\ \mathrm{eV},$$

$$\mathrm{Ru}: \theta_{\mathrm{Cs}} \sim 5.3 \times 10^{14}\ \mathrm{Cs/cm^2}, \quad \Phi = 2\ \mathrm{eV},$$

$$\mathrm{Ag}: \theta_{\mathrm{Cs}} \sim 4.6 \times 10^{14}\ \mathrm{Cs/cm^2}, \quad \Phi = 1.6\ \mathrm{eV}$$

close to the photoemission maxima in each case.

In this work we have carried out direct measurements on Cs-dosed Au(111) surfaces; deriving results for both the work function and the Cs coverage using visible and x-ray photoelectron spectroscopy[11] (XPS) detected by a hemispherical electron energy analyzer. We find that the work function of Cs-dosed Au(111) prepared by the method described above and in Ref. 2 is 1.61 ± 0.08 eV with a Cs coverage of $(3.0–4.9) \times 10^{14}$ cm^{-2}.

II. EXPERIMENTAL

The experiments were performed in an ultrahigh vacuum (UHV) chamber (10^{-10} Torr base pressure) at the Stanford Synchrotron Radiation Laboratory. The chamber was connected to synchrotron beam line 8-1 with the ability to produce soft x-ray light with photon energies between 30 and 170 eV. A spherical electron energy analyzer (PHI model 10-360) mounted on the chamber was used to record photoelectron spectra. The vacuum system was equipped with a commercially available Cs source (SAES Getters), which contains a cesium chromate salt that emits Cs atoms when heated. The Cs deposition onto a Au(111) surface was performed by running 5.5 A through the doser confined within a molybdenum "can" with a 1 mm shuttered opening. The Cs deposition was monitored by measuring the photoemission current when the sample was exposed to light from a 632.8 nm (1.96 eV photon energy) HeNe laser (0.95 mW, 1 mm spot size) until the photoemission current reached a maxi-

a)Electronic mail: wodtke@chem.ucsb.edu.

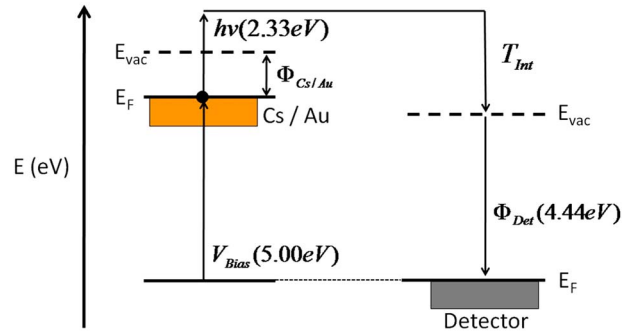

FIG. 1. (Color online) Energy diagram of a photoelectron. It is initially excited by a photon ($h\nu$) into vacuum and then accelerated by a 5 V bias. The kinetic energy of the electron must be large enough to overcome the work function of the detector. The energy that is measured is the internal kinetic energy (T_{int}).

mum. The Au(111) sample was prepared for Cs dosing by heating to 200 °C for 1 h and then examined with XPS (130 eV photon energy) to ensure that all trace amounts of Cs had been removed from the surface.

For work function measurements of the cesiated sample, two different lasers were directed onto the sample and the energy distribution of the photoelectrons was measured using the electron energy analyzer at 5 min intervals over 130 min after Cs deposition. We monitored the work function over this period to measure the stability of the surface. The second laser was a frequency doubled neodymium-doped yttrium aluminum garnet, which produced 5 mW of continuous power at 532 nm (2.33 eV photon energy). For electron detection, a −5 V bias was applied to the surface to overcome the energy barrier created by the work function difference between the sample and the detector. Figure 1 is an energy diagram depicting the detection of the photoelectrons.

XPS was used to derive information about the coverage of Cs atoms on the Au(111) surface by analyzing the core level spectroscopy of the surface. Photon energies of 120 and 130 eV were used to probe the Au 4*f* and Cs4*d* core levels. The peak intensities were analyzed using the software AAnalyzer.[12] To ensure accurate results, all XPS measurements on cesiated samples were taken within minutes after Cs dosing.

III. RESULTS AND ANALYSIS

A. Visible photoelectron spectroscopy: Determination of the work function

As the detector and sample are both referenced to the ground, in the absence of a bias, their Fermi energies are equal. Since the work function of the detector is ~2.8 eV larger than that of the sample, a potential barrier exists that the photoelectrons must overcome to be detected, so a −5 V bias is applied to the surface to overcome this barrier (see Fig. 1). To account for the fact that the measured kinetic energy of the photoelectrons depends on the detector work function and the −5 V bias, the term internal kinetic energy is used, T_{int}, which may be thought of as the apparent kinetic energy. $T_{\text{int}}^{\text{max}}$ is the maximum internal kinetic energy of the photoelectron energy distributions, while $T_{\text{int}}^{\text{min}}$ is the minimum internal kinetic energy where the electrons have barely

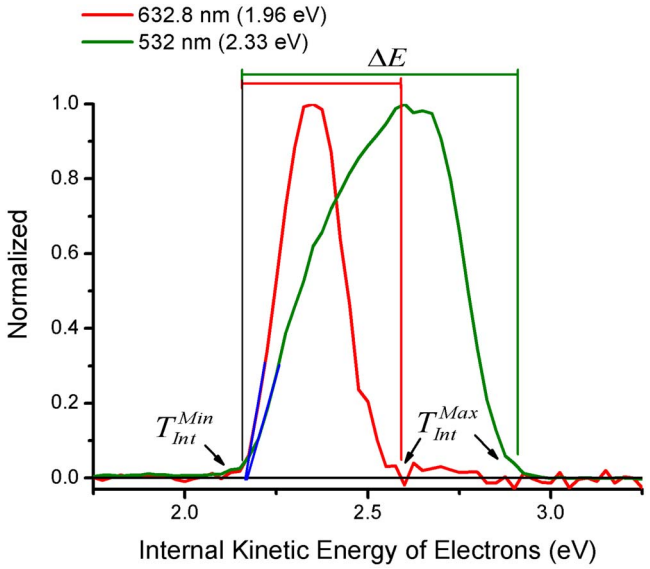

FIG. 2. (Color online) Photoelectron energy distribution of a cesiated Au(111) sample from 632.8 and 532 nm lasers. The work function of the surface ($\Phi_{\text{Cs/Au}}$) is found by subtracting ΔE from the energy of the photon. The value of the internal kinetic energy of electrons where the blue lines intersect the x axis determines the value of $T_{\text{int}}^{\text{min}}$.

enough energy to escape the surface, as is shown in Fig. 2. More explicitly, $T_{\text{int}}^{\text{max}}$ and $T_{\text{int}}^{\text{min}}$ can be defined by

$$T_{\text{int}}^{\text{max}} = h\nu + V - \Phi_{\text{det}}, \tag{1}$$

$$T_{\text{int}}^{\text{min}} = V + \Phi_{\text{Cs/Au}} - \Phi_{\text{det}}, \tag{2}$$

where $h\nu$ is the photon energy, V is the applied bias voltage, Φ_{det} is the work function of the detector, and $\Phi_{\text{Cs/Au}}$ is the work function of the sample. As can be seen from Eq. (1), $T_{\text{int}}^{\text{max}}$ is independent of $\Phi_{\text{Cs/Au}}$ and can be used to derive Φ_{det}. This makes the work function easily obtainable by solving for $\Phi_{\text{Cs/Au}}$ in Eq. (2):

$$\Phi_{\text{Cs/Au}} = T_{\text{int}}^{\text{min}} - V + \Phi_{\text{det}}. \tag{3}$$

Furthermore, Eq. (1) can be plugged into Eq. (3) resulting in

$$\Phi_{\text{Cs/Au}} = h\nu - (T_{\text{int}}^{\text{max}} - T_{\text{int}}^{\text{min}}) = h\nu - \Delta E, \tag{4}$$

where ΔE is the width of the photoelectron energy distribution.

Figure 2 shows the photoelectron energy distribution of the cesiated sample using both the 632.8 and 532 nm lasers. The spectra have been normalized for direct comparison. $T_{\text{int}}^{\text{min}}$ can be determined analytically from electron energy distribution spectra like those shown in Fig. 2. The small tail associated with $T_{\text{int}}^{\text{min}}$ in the spectra is an artifact of the detector, which obscures the low energy end of the curves.[13] The maximal error associated with this source of uncertainty is 0.06 eV. The error associated with the determination of $T_{\text{int}}^{\text{max}}$ is smaller than this. The work function of the freshly cesiated surface was found from analysis of data like those shown in Fig. 2 to be 1.61 ± 0.08 eV independent of the choice of laser. These results are consistent with wavelength dependent photoemission yield spectra that have been previously reported.[14]

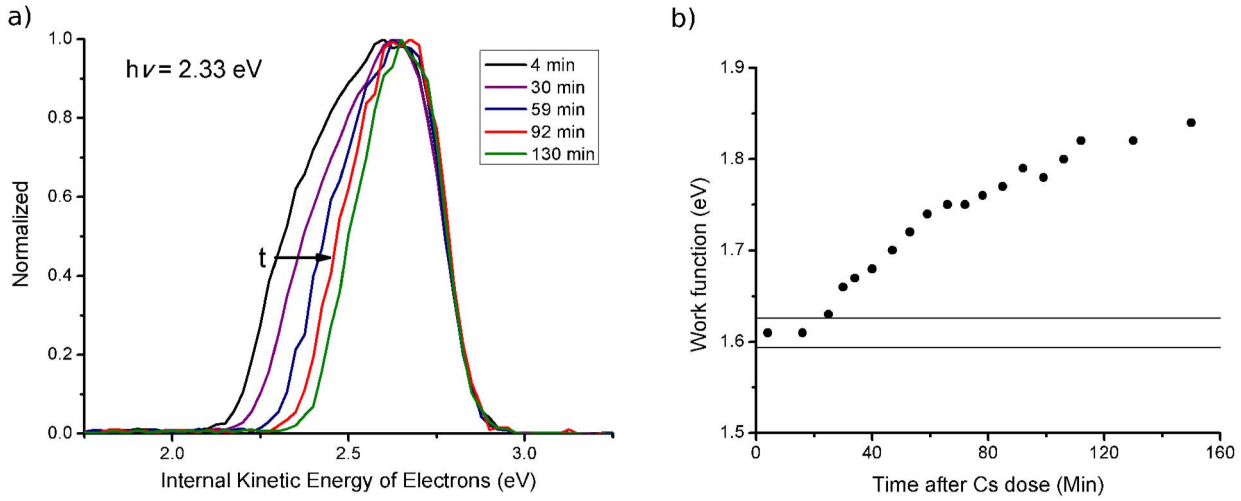

FIG. 3. (Color online) (a) The photoelectron energy distribution as a function of time after Cs dosing. As time increases, ΔE ($T_{\text{int}}^{\max} - T_{\text{int}}^{\min}$) becomes smaller, giving a larger value for the work function, $\Phi_{\text{Cs/Au}}$. (b) The work function of the cesiated Au(111) surface ($\Phi_{\text{Cs/Au}}$) as a function of time after dosing. After 130 min, the work function increases by 0.2 eV, or roughly one vibrational quanta of energy for NO.

We now consider how the work function of the cesiated surface changes over time using the 532 nm laser. This can be easily observed by monitoring the change in the width of the internal kinetic energy distribution at various times after Cs deposition. See Fig. 3(a). Figure 3(b) shows the derived work function versus time. Note that we observe a 15% change in the work function over the course of 130 min from its initial value of 1.61 to 1.84 ± 0.08 eV at a base pressure of 1×10^{-10} Torr. The cause of this slow change in work function is not known, but we speculate that background gas in the UHV chamber slowly oxidizes the surface. Also shown as horizontal lines in Fig. 3(b) are $\pm 1\%$ variations in the determined work function. This characterization of the stability of Cs/Au surfaces validates previous methods used to observe vibrationally promoted electron emission, where all data were obtained within 20 min of preparation at a similar base pressure.[2–4]

B. X-ray photoelectron spectroscopy: The coverage of Cs at maximum photoemission

Although not the major goal of this work, we did obtain some data relevant to the determination of the Cs coverage at maximum photoemission on Au(111) and we report the interpretation of those data here. Our data were of three forms. Various surface probes are used to compare Cs on Au(111) to other Cs adlayer systems, specifically Cs on GaAs, whose Cs coverage has been characterized before,[15–18] and Cs on InP, which is expected to behave similarly to GaAs. First, we made direct comparisons of dosing times necessary to achieve maximum photoemission coverage on Au(111) and InP(100). Second, we compared Cs XPS feature intensities for Cs on Au(111) to Cs on InP(100). Finally, by fixing the x-ray source on a Au spectral feature and measuring photoelectron emission intensity attenuation induced by Cs dosing, we compare Cs on Au(111) to Cs on GaAs.

We now review the state of knowledge on the quantitative Cs surface density on GaAs—and by inference, InP, which is summarized in Table I. Goldstein[15] used Auger electron spectroscopy (AES) monitoring the 47 eV Cs peak intensity to measure relative Cs coverages on GaAs(100) and GaAs(111) *A* and *B* faces. These results were calibrated against identical control experiments for Cs on Ge(100), where a structural model for the ordered Cs overlayers that produced a 2×2 low-energy electron diffraction (LEED) pattern could be used to calculate a precise coverage.[16] Goldstein[15] used an observed inflection point in the AES-monitored dosing curve for GaAs(100), after which Cs adsorption was much slower (under the same dosing flux) to identify the dosing time for a saturated layer of Cs on GaAs(100). Goldstein[15] also noted that the dosing inflection point occurred where the LEED pattern of the underlying GaAs disappeared. This analysis suggests that the saturated Cs coverage on GaAs(100) occurs for a Cs surface density of 7.2×10^{14} Cs cm^{-2}. By assuming that the sticking coefficient of Cs to GaAs was independent of coverage, Goldstein[15] was able to linearly extrapolate to the coverage at maximum photoemission, which was reported to be 3.6×10^{14} Cs cm^{-2}.

van Bommel *et al.*[20] also used the Cs 47 eV feature from AES in a similar fashion to that of Goldstein[15] and also reported an inflection point. In contrast to Goldstein's[15] work, this "break point" was reported to occur at the photoemission maximum. This experiment was calibrated by comparing Cs Auger signals observed from surfaces with well defined LEED patterns resulting from ordered overlayers of Cs on GaAs(110) and GaAs($\bar{1}\bar{1}\bar{1}$). This led to the conclusion that the maximum photoemission Cs coverage on GaAs(100) is 5.3×10^{14} Cs cm^{-2}.[20] Clearly this calibration procedure produced different results than that of Goldstein.[15] In this analysis, the 4×4 Cs overlayer on GaAs(110) used for calibration was believed to exhibit a surface density of 4.7×10^{14} Cs cm^{-2}. More recently scanning tunnel microscopy (STM) images of this ordered overlayer have been reported.[21] By "counting atoms" in representative STM images, one may calculate that the actual surface density of this overlayer would be 4.0×10^{14} Cs cm^{-2}, assuming a perfect

TABLE I. Important papers relating to the Cs atom surface density on GaAs at maximum photoemission.

Derived Cs atom surface density (atoms cm^{-2}) (photoemission maximum)	Derived Cs atom surface density (atoms cm^{-2}) (saturation coverage)	Literature
$(5.2–6.9)\times10^{14}$; possibly as low as 4×10^{14} due to roughness	Not determined	[a]
3.6×10^{14}	7.2×10^{14}	[b]
5.3×10^{14}	7.9×10^{14}	[c]
5.3×10^{14}	Not determined	[d]
4.1×10^{14} [e]	6.1×10^{14} [e]	[c]
4.1×10^{14} [e]	Not determined	[d]

[a]Reference 17.
[b]References 15 and 16.
[c]Reference 19.
[d]Reference 20.
[e]By using a calibration based on STM atom counting from Ref. 21. See text.

overlayer. The STM images of Ref. 21 clearly show vacancy defects, perhaps better described as disorder vacancies. We estimate that this lowers the Cs surface density by an additional 10%, meaning that the 4×4 overlayer on GaAs(110) actually exhibits a Cs surface density as low as 3.6×10^{14} Cs cm^{-2}. We have used this value to recalibrate the results of van Bommel *et al.*,[20] which bring it closer in agreement with those of Goldstein;[15] namely, we find the maximum photoemission coverage to be 4.1×10^{14} Cs cm^{-2}.

Rodway[19] used the Cs 563 eV AES peak intensity as a function of Cs dosing time in similar experiments to those of Goldstein[15] and van Bommel *et al.*[20]. In this work, *two* inflection points in the dosing curves were observed.[19] The first inflection point was found to be coincident with the photoemission maximum. The second of these was assigned to be the saturated coverage inflection seen by Goldstein.[15] Rodway[19] concluded that the saturation coverage was 7.9×10^{14} Cs cm^{-2} and the maximum photoemission coverage was 5.3×10^{14} Cs cm^{-2},[19] adopting the calibration results of van Bommel *et al.*[20] If we recalibrate this result based on STM atom counting, we again obtain a maximum photoemission coverage of 4.1×10^{14} Cs cm^{-2} and saturation coverage of 6.1×10^{14} Cs cm^{-2}.

Finally and in a very different study, Sommer *et al.*[17] dosed epitaxially grown GaAs thin films with Cs to the photoemission maximum of a white light (W filament) light source. They then dissolved the sample in acid and analyzed Cs concentrations by absorption spectroscopy. They reported surface densities between 5.2 and 6.9×10^{14} Cs cm^{-2}. However, they noted that due to GaAs surface roughness, the Cs atom surface density might be as low as 4×10^{14} Cs atom cm^{-2}.

A summary of this literature review is shown in Table I. From the work of Goldstein[15] and the recalibrated work of Rodway[19] and van Bommel *et al.*,[20] we conclude that a saturation layer of Cs on GaAs is in the range of $(6.1–7.2)\times10^{14}$ cm^{-2}, and that the surface of maximum photoemission exhibits a Cs coverage of $(3.6–4.1)\times10^{14}$ cm. As InP exhibits a lattice constant only 7% different than that of GaAs and its surface chemistry is expected to be similar to that of GaAs, we assume that these numbers also apply to InP, at least within the range of uncertainty shown above.

To obtain coverages of Cs on Au(111), we have also compared Cs dosing times to maximum photoemission for Au(111) and InP(100). Under reasonably well controlled conditions, we find that the dosing times differ by less than a few percent: $\tau_{Au}=0.96\tau_{InP}$. Assuming the sticking coefficient to be unity in both cases over this dosing range, we conclude that the Cs surface densities at maximum photoemission are similar for these two surfaces. This approach leads to a derived Cs coverage at maximum photoemission on Au(111) of $(3.4–3.9)\times10^{14}$ Cs cm^{-2} or 0.25–0.28 ML.

In the second experiment, we compared the relative integrated XPS intensity of the Cs 4*d* lines for dosing to maximum photoemission on Au(111) to that obtained by dosing on InP(100). These results also suggest that the Cs atom surface density is similar on these two surfaces. More specifically, we derive a coverage of $(3.0–3.5)\times10^{14}$ cm^{-2} or 0.21–0.25 ML.

Finally, we compared photoelectron emission attenuation from Au core levels when dosed with Cs to that from As and Ga core levels also under controlled Cs dosing conditions. If one assumes the same attenuation lengths on the two surfaces, one may obtain the Cs coverage in this way. On the Au(111) surface dosed to maximum photoemission, we observe an attenuation of 0.48 ± 0.03 when monitoring photoelectrons produced by the Au 4*f* XPS feature ($eKE\approx39$ eV).[22] This can be compared to experiments where Cs is dosed on GaAs(100) to saturation coverage, in which the Ga 3*d* ($eKE\approx96$ eV) and As 3*d* ($eKE\approx74$ eV) integrated intensities are attenuated to 0.48–0.58 of their original values.[18] Thus the apparent Cs-atom surface density on Au(111) is in the range of 0.8–1.0 that of a Cs saturated GaAs(100) surface, based on attenuation of photoelectrons. Note that the attenuation does not depend strongly on electron energy in this energy range. For example, similar experiments to these have been carried out on Cs adlayers on InP, in which the P 2*p* ($eKE\approx33$ eV) and In 4*d* ($eKE\approx99$ eV) integrated intensities are attenuated to 0.48 and 0.44 of their original values, respectively, by a saturation layer of Cs.[23] This comparison suggests the maximum photoemission Cs surface density on Au(111) of $(4.9–7.2)\times10^{14}$ cm^{-2}, that is, 0.35–0.51 ML.

Despite the relatively large uncertainties, it is worth comparing these results to a number of Cs adlayer systems,

TABLE II. Comparison of several substrate surfaces dosed with Cs to maximum photoemission.

Metal	θ_{Cs} (cm^{-2})	θ_M [a] (cm^{-2})	ML	Φ (eV)	Φ_M (eV)	$\Delta\Phi$ (eV)
W	2.5×10^{14}	1.29×10^{15}	0.19	1.5	4.41	2.9
Ru(0001)	5.3×10^{14}	1.62×10^{15}	0.33	2	4.7	2.7
Ag(111)	4.6×10^{14}	1.39×10^{15}	0.33	1.65	4.73	3.1
Au(111)	$(4.9-7.2)\times10^{14}$ or $(3.4-3.9)\times10^{14}$ or $(3.0-3.5)\times10^{14}$	1.39×10^{15}	0.35–0.51[b] or 0.25–0.28[c] or 0.22–0.25[d]	1.61	5.1	3.5
GaAs(100)	$(3.6-4.1)\times10^{14}$	1.27×10^{15}	0.28–0.32			
InP(100)	$(3.6-4.1)\times10^{14}$	1.16×10^{15}	0.30–0.35			

[a]For InP and GaAs, the surface density refers to all atoms and does not reflect the details associated with surface reconstruction.
[b]Based on photoelectron attenuation and comparison to Cs dosing on GaAs(100).
[c]Based on comparative dosing times to maximum photoemission for InP(100).
[d]Based on relative Cs XPS intensity measurements comparing Au(111) to InP(100).

shown in Table II. One can see that the results obtained here are consistent with this comparison group. Although uncertainties persist—in particular, the error associated with the attenuation experiments is not explained—we conclude that the Cs coverage on Au(111) at maximum photoemission is in the range of $(3.0-4.9)\times10^{14}$ cm^{-2} or 0.22–0.35 ML, which is consistent with the comparison group. Additional experiments, for example, using STM to image Cs on Au(111) after controlled doses, could be used to reduce the uncertainty of this coverage determination.

The derived Cs coverage and simple chemical arguments place some constraints on reasonable structural models for this Cs/Au surface. It is understood that when Cs bonds to a gold surface, a partial charge transfer occurs from the Cs to Au, leaving Cs positively charged.[7] As the maximum photoemission is observed close to the work function minimum, we expect this structure to represent a maximal surface dipole that can be produced by this bonding mechanism. Thus, it is useful to compare the ionic radius of Cs^+ (1.8 Å), which represents a minimum size of Cs on Au, the van der Waals radius of Cs (3.1 Å), which represents a maximum size of Cs on Au, and the Au–Au nearest neighbor spacing on the 111 surface (2.88 Å). A maximal surface dipole is obtained by balancing two factors. In the low coverage limit, bonding additional Cs atoms lead to a large fractional charge transfer from Cs to Au, but as more Cs is added, dipolar repulsion arises, reducing charge transfer and increasing the effective size of the Cs. At higher coverages, charge transfer becomes less likely and Cs–Cs bonding begins to become more energetically favorable and a second Cs layer will eventually grow.

Assuming one limiting case, where Cs^+ binds to Au(111) with complete transfer of a single charge, the ratio of surface areas of a Cs^+ atom to Au atom would result in a maximal coverage prediction of

$$\text{Ionic limit} - \left(\frac{2.88}{3.6}\right)^2 = 0.64 \text{ ML} = 8.9\times10^{14} \text{ Cs/cm}^2.$$

Similarly, assuming no charge transfer, the ratio of a neutral Cs to Au atom would result in a coverage prediction of

$$\text{Neutral limit} - \left(\frac{2.88}{6.2}\right)^2 = 0.22 \text{ ML} = 3.1\times10^{14} \text{ Cs/cm}^2.$$

The reported Cs coverage of about $(3.0-4.9)\times10^{14}$ Cs cm^{-2} (0.4–0.5 ML) lies midway between these limits, suggesting partial charge transfer.

It is particularly interesting to compare these findings to that of a similar system, the monolayer saturation coverage of Cs on Ag(111) (0.33 ML). The lattice constant of Ag is nearly identical to that of Au and both are strongly electronegative. For Ag, the Cs adsorbs on the hcp hollow sites with a $\sqrt{3}\times\sqrt{3}$ structure and a Cs–Cs distance of 5.01 Å (a coverage corresponding to 4.6×10^{14} Cs cm^{-2}).[10] As the atom-atom spacing on Au(111) is nearly identical to that on Ag(111), we might expect a nearly identical predicted coverage of -4.6×10^{14} Cs cm^{-2}, if we were to postulate that the same $\sqrt{3}\times\sqrt{3}$ structure well represented the *HeNe-maximum-photoemission* Cs/Au surface. Indeed, this is consistent with our observations.

Lastly, we would like to mention one interesting feature of the Cs 4*d* peaks in Fig. 4. These peaks exhibit a doubled structure, which has been previously observed albeit at lower resolution.[24] The peaks at 50 and 47.7 eV (solid lines) should be compared to the peaks at 49.1 and 46.9 eV (dashed lines). The 2.3 eV splitting of the solid and dashed lines is due to the spin orbit effect in the Cs atom, i.e., the difference between Cs $4d_{5/2}$ and Cs $4d_{3/2}$. However, the origin of the further doubling of the spin-orbit split peaks is subject to further inquiry. It is possible that Cs atoms occupy two different types of surface sites and thus have different charge transfers to the Au surface; however, it does not seem that this influence could give rise to such a large shift. Another possibility is that the double peak structure arises from some surface reaction, for example, Cs diffusion into Au, related to incipient Cs–Au alloy formation.[14,24,25] STM studies of alkali

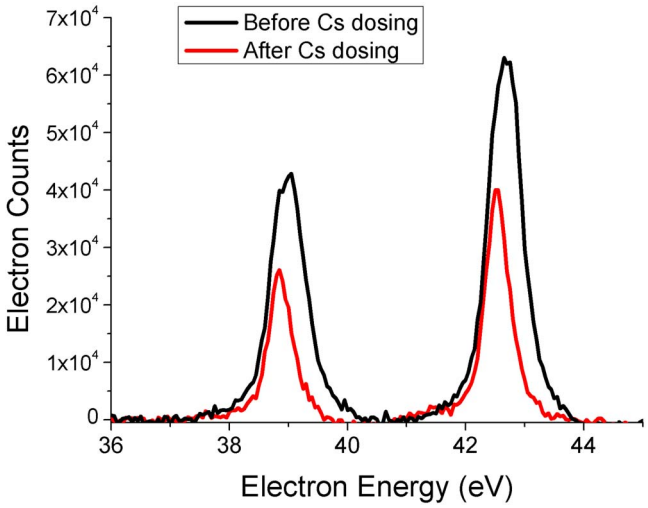

FIG. 4. (Color online) Attenuation of the Au 4*f* XPS peaks. The red peaks are the photoelectron energy distribution of the Au 4*f* XPS peaks before dosing and the black peaks are after Cs dosing. The background has been subtracted from the data for better comparison.

atoms on Au(111) show surface structures that are sufficiently diverse to possibly lead to bimodal XPS lines.[26] This is perhaps also consistent with the small shift in the Au 4*f* lines apparent upon Cs dosing. See Fig. 5. Experiments at higher temperatures, a wider variety of dosing conditions, and the use of additional surface analytical techniques such as LEED and STM will be needed to fully understand this phenomenon.

IV. CONCLUSION

The results of these measurements show a work function of $\varphi = 1.61 \pm 0.08$ eV for a Cs-covered Au surface at the maximum HeNe laser photoemission. We presented results from three different sets of measurements, suggesting the Cs coverage on this surface. The results for the work function are consistent with but much more accurate than previous estimates made for this surface and we hope they will serve to provide a better basis for evaluating theoretical interpretations on vibrationally promoted electron emission.

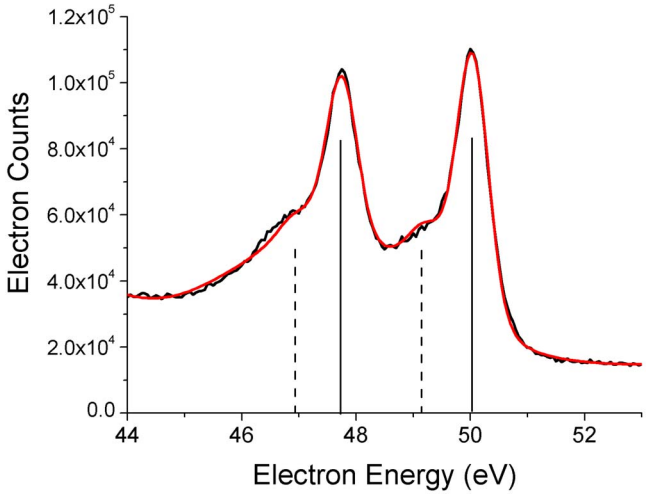

FIG. 5. (Color online) Photoelectron energy distribution of the Cs 4*d* XPS peaks after Cs dosing.

ACKNOWLEDGMENTS

We gratefully acknowledge the financial support from the National Science Foundation under Grant No. CHE-0454806 and the Partnership for International Research and Education—for Electronic Chemistry and Catalysis at Interfaces—NSF Grant No. OISE-0530268. N.H.N. acknowledges financial support through a Feodor–Lynen Fellowship provided by the Alexander von Humboldt Foundation. Portions of this research were carried out at the Stanford Synchrotron Radiation Laboratory, a national user facility operated by Stanford University on behalf of the U.S. Department of Energy, Office of Basic Energy Sciences.

[1] A. M. Wodtke, D. Matsiev, and D. J. Auerbach, Prog. Surf. Sci. **83**, 167 (2008).
[2] J. D. White, J. Chen, D. Matsiev, D. J. Auerbach, and A. M. Wodtke, Nature (London) **433**, 503 (2005).
[3] J. D. White, J. Chen, D. Matsiev, D. J. Auerbach, and A. M. Wodtke, J. Chem. Phys. **124**, 064702 (2006).
[4] J. D. White, J. Chen, D. Matsiev, D. J. Auerbach, and A. M. Wodtke, J. Vac. Sci. Technol. A **23**, 1085 (2005).
[5] M. Silva, R. Jongma, R. W. Field, and A. M. Wodtke, Annu. Rev. Phys. Chem. **52**, 811 (2001); A. M. Wodtke, J. C. Tully, and D. J. Auerbach, Int. Rev. Phys. Chem. **23**, 513 (2004).
[6] Y. H. Huang, C. T. Rettner, D. J. Auerbach, and A. M. Wodtke, Science **290**, 111 (2000); A. M. Wodtke, Y. H. Huang, and D. J. Auerbach, J. Chem. Phys. **118**, 8033 (2003).
[7] R. D. Diehl and R. McGrath, J. Phys.: Condens. Matter **9**, 951 (1997).
[8] C. S. Wang, J. Appl. Phys. **48**, 1477 (1977).
[9] G. Ertl, A. Böttcher, and A. Morgante, Surf. Sci. Lett. **359**, L461 (1996); T. Greber, R. Grobecker, A. Morgante, A. Bottcher, and G. Ertl, Phys. Rev. Lett. **70**, 1331 (1993).
[10] G. S. Leatherman and R. D. Diehl, Phys. Rev. B **53**, 4939 (1996); M. Caragiu, G. S. Leatherman, R. D. Diehl, P. Kaukasoina, and M. Lindroos, Surf. Sci. **441**, 84 (1999).
[11] J. F. Watts and J. Wolstenholme (unpublished).
[12] A. Herrera-Gómez, P. Pianetta, D. Marshall, E. Nelson, and W. E. Spicer, Phys. Rev. B **61**, 12988 (2000).
[13] F. G. Allen and G. W. Gobeli, Phys. Rev. **144**, 558 (1966).
[14] M. V. Knat'ko, M. N. Lapushkin, and V. I. Paleev, Tech. Phys. Lett. **24**, 390 (1998); M. V. Knat'ko, M. N. Lapushkin, and V. I. Paleev, Phys. Low-Dimens. Semicond. Struct. **9–10**, 57 (2001).
[15] B. Goldstein, Surf. Sci. **47**, 143 (1975).
[16] B. Goldstein and R. U. Martinelli, J. Appl. Phys. **44**, 4244 (1973).
[17] A. H. Sommer, H. H. Whitaker, and B. F. Williams, Appl. Phys. Lett. **17**, 273 (1970).
[18] Z. Liu, Ph.D. thesis, 2005.
[19] D. Rodway, Surf. Sci. **147**, 103 (1984).
[20] A. J. van Bommel, J. E. Crombeen, and T. G. J. van Oirschot, Surf. Sci. **72**, 95 (1978).
[21] L. J. Whitman, J. A. Stroscio, R. A. Dragoset, and R. J. Celotta, Phys. Rev. Lett. **66**, 1338 (1991).
[22] *eKE* is an abbreviation for electron kinetic energy.
[23] Y. Sun, Z. Liu, and P. Pianetta, J. Vac. Sci. Technol. A **25**, 1351 (2007); S. Tanuma, C. J. Powell, and D. R. Penn, Surf. Interface Anal. **36**, 1 (2004).
[24] G. K. Wertheim, J. E. Rowe, C. M. Chiang, R. A. Malic, and D. N. E. Buchanan, Surf. Sci. **330**, 27 (1995).
[25] M. Skottkeklein, A. Bottcher, R. Imbeck, S. Kennou, A. Morgante, and G. Ertl, Thin Solid Films **203**, 131 (1991).
[26] J. V. Barth, R. Schuster, R. J. Behm, and G. Ertl, Surf. Sci. **348**, 280 (1996); J. V. Barth, R. J. Behm, and G. Ertl, *ibid.* **341**, 62 (1995); J. V. Barth, R. J. Behm, and G. Ertl, *ibid.* **302**, L319 (1994); J. V. Barth, H. Brune, R. Schuster, G. Ertl, and R. J. Behm, *ibid.* **292**, L769 (1993).